

Efficient Charge Transport in Semisynthetic Zinc Chlorin Dye Assemblies

Sameer Patwardhan,^{†,‡} Sanchita Sengupta,^{‡,§} Laurens D. A. Siebbeles,[†] Frank Würthner,^{*,‡} and Ferdinand C. Grozema^{*,†}

[†]Optoelectronic Materials Section, Department of Chemical Engineering, Delft University of Technology, Julianalaan 136, 2628 BL, Delft, The Netherlands

[‡]Universität Würzburg, Institut für Organische Chemie and Center for Nanosystems Chemistry, Am Hubland, 97074 Würzburg, Germany

S Supporting Information

ABSTRACT: We have studied the charge transport properties of self-assembled structures of semisynthetic zinc chlorins (ZnChls) in the solid state by pulsed radiolysis time-resolved microwave conductivity measurements. These materials can form either a two-dimensional (2D) brickwork-type slipped stack arrangement or a one-dimensional (1D) tubular assemblies, depending on the exact molecular structure of the ZnChls. We have observed efficient charge transport with mobilities as high as $0.07 \text{ cm}^2 \text{ V}^{-1} \text{ s}^{-1}$ for tubular assemblies of 3¹-hydroxy ZnChls and up to $0.28 \text{ cm}^2 \text{ V}^{-1} \text{ s}^{-1}$ for 2D stacked assemblies of 3¹-methoxy ZnChls at room temperature. The efficient charge transporting capabilities of these organized assemblies opens the way to supramolecular electronics based on biological systems.

Natural functional architectures, such as secondary and tertiary structures of proteins, cyclic chlorophyll arrays in light-harvesting complexes, and π -stacked structure of double-stranded DNA, provide inspiration for the rational design of structural motifs that are promising for supramolecular electronics.^{1–3} There are many representative examples of self-assembling materials, including discotic liquid crystals (DLCs),^{2,4,5} tapes,⁶ zippers,⁷ well-defined π -stacks,⁸ and self-assembled nanorods and nanotubes based on various π -conjugated molecules.^{9–12} However, true biomimetic self-assembled materials that have properties relevant for supramolecular electronics are rare.

Green sulfur and non-sulfur photosynthetic bacteria have unique chlorosomal antenna systems to harvest sunlight with quantum efficiencies close to unity.^{13–15} The chlorosomal antennae are constructed from bacteriochlorophyll (BChl) pigments that are held together in the proper geometrical arrangement by non-covalent interactions, without stabilization by a protein matrix.^{16–19} These systems provide an inspiration for the rational design of one-dimensional (1D) supramolecular architectures with desirable properties for opto-electronics and artificial photosynthesis.

Working toward this goal, we have studied the charge transport properties of semisynthetic BChl *c* derivatives, namely, zinc chlorins (ZnChls). For these compounds, the supramolecular organization, particularly in the solid state, has

been elucidated by solid-state NMR measurements previously.²⁰ Here we report efficient charge transport in semisynthetic ZnChls using pulsed radiolysis time-resolved microwave conductivity (PR-TRMC) measurements.

Over the past few years, some of us have shown that the *in vitro* self-assembly of natural BChls can be effectively influenced by simple chemical modifications.^{20–25} For instance, the use of a Zn ion instead of Mg ion imparts chemical stability,²⁶ the solubility properties can be tailored by the 17²-side chain, and the stacking mode is controlled by the 3¹-functionality and/or 17²-side chain (see Figure 1). Most notably, it has been shown previously that the self-assembly paths of 3¹-hydroxy- and 3¹-methoxy-functionalized ZnChls derived from BChl *c* are very different. The 3¹-hydroxy derivatives were shown to assemble

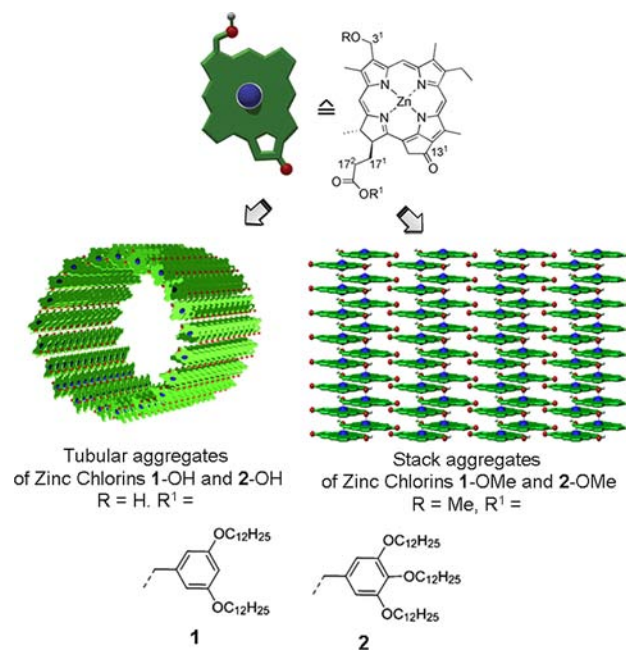


Figure 1. Chemical structures and self-assembled architectures of semisynthetic 3¹-hydroxy (1-OH, 2-OH) and 3¹-methoxy (1-OMe, 2-OMe) zinc chlorins investigated in this work.

Received: July 31, 2012

Published: September 18, 2012

into tubular structures,^{23,24} while the 3¹-methoxy analogues form two-dimensional (2D) sheet-like structures.²⁰ The self-assembly of these compounds has been studied in solution,^{21,23,24,27} on surfaces,^{22,25} and in the solid state.²⁰ In a recent study, we reported high conductivity of 0.48 S m⁻¹ along single tubes consisting of 3¹-hydroxy ZnChls on a micrometer length scale by the conductive atomic force microscopy technique, while a charge carrier mobility of 0.03 cm² V⁻¹ s⁻¹ in the solid state was determined by PR-TRMC.²⁴ The mobility of charges in organic semiconductors is intimately related to the supramolecular organization that is often difficult to control in soft materials.²⁸ Therefore, it is of considerable interest to establish how the differences in the supramolecular structure for the 3¹-hydroxy and 3¹-methoxy ZnChls affect the mobility of charges in these materials.

In order to achieve this, semisynthetic 3¹-hydroxy ZnChls (1-OH, 2-OH) and 3¹-methoxy ZnChls (1-OMe, 2-OMe; Figure 1) were synthesized by stepwise derivatization of chlorophyll *a*. The synthesis and detailed structural characterization have been reported previously,^{20–23,25} and additional characterization is provided in the Supporting Information. In both the OMe and OH compounds, the combination of π – π stacking of the chlorin cores and coordination of the central zinc ion with the 3¹-hydroxy or 3¹-methoxy group of a neighboring molecule leads to the formation of slipped stacked structures with J-type excitonic coupling.²⁹ For OH ZnChls, higher-order tubular structures can be formed upon self-assembly in solution in which these stacks are held together by hydrogen bonds between the 3¹-hydroxy group and the 13¹-keto functionality (see Figure 1). In the absence of interstack hydrogen-bonding, the 3¹-methoxy ZnChls form 1D stacks that are further organized into a brickwork-type 2D sheets.²⁰

The charge transport properties of the OH and OMe ZnChls were studied by PR-TRMC to obtain the charge carrier mobility in the solid state.³⁰ In this technique, the change in conductivity of a material is measured upon irradiation with a short nanosecond pulse of high-energy electrons. Details on the technique and analysis of the data are given in the Supporting Information. In Figure 2, the change in conductivity ($\Delta\sigma$) per unit of the deposited energy (*D*) is shown as a function of time for all materials considered here. The conductivity initially increases during the 10 ns irradiation pulse due to the creation of mobile charge carriers. Subsequently, the conductivity decays as a result of recombination and/or trapping of charges after the generating pulse. As is evident from Figure 2, there are distinct differences in the magnitude and the lifetime of the conductivity signals for the OH and OMe ZnChls. For both OMe compounds, a high conductivity signal is observed that decays back to zero within \sim 200 ns, while for the OH compounds the end-of-pulse value of the conductivity is roughly a factor of 4 lower but the lifetime is considerably longer. Both compounds 1 and 2 with different side chains on the 17²-position give similar trends, as is evident from Figure 2, although the absolute conductivity values for both the OMe and OH varieties of 2 are significantly lower than for 1.

The mobility of charges can be calculated from the conductivities at the end of the pulse if the concentration of charges is known. The concentrations of charges were estimated using the charge-scavenging model described previously.³¹ The values for the mobility obtained in this way are included in Figure 2. The OMe ZnChls exhibit significantly higher mobilities (up to 0.28 cm² V⁻¹ s⁻¹) than the corresponding OH compounds (up to 0.07 cm² V⁻¹ s⁻¹). For

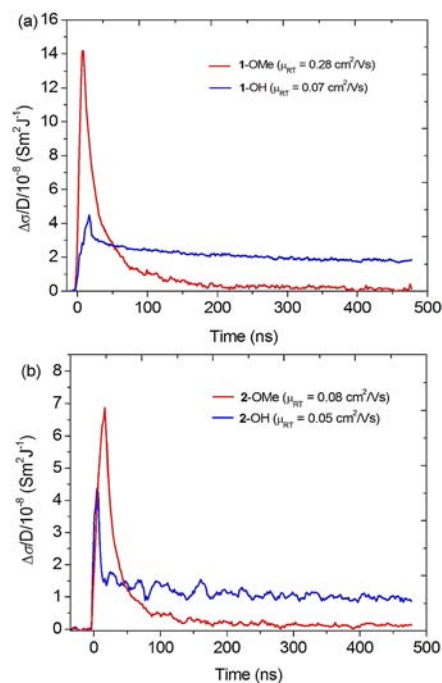


Figure 2. Transient change in conductivity of ZnChls upon irradiation with a 10 ns electron pulse: (a) 1-OH, 1-OMe; (b) 2-OH, 2-OMe.

the OH compounds, the mobilities found here are of the same order of magnitude as the recently reported value of 0.03 cm² V⁻¹ s⁻¹ in tubular OH-substituted ZnChls containing hydrophilic side chains.²⁴ The mobility values reported here, 0.05–0.28 cm² V⁻¹ s⁻¹, are comparable to values typically obtained for DLCs, with the highest value approaching the record published for DLCs (\sim 1 cm² V⁻¹ s⁻¹).³²

Interestingly, for previously studied DLC porphyrins that have a similar core structure, mobilities in the same range, \sim 0.05–0.40 cm² V⁻¹ s⁻¹, were found.³¹ However, in these materials, the planar porphyrin cores form columnar structures with little lateral shift with respect to each other. This leads to effective π -stacking and larger average overlap between neighboring molecules. In ZnChls, the zinc–oxygen coordination directs the molecules into slipped stacking arrangements where the π -overlap is smaller. Apparently, the coordinative bond, combined with the steric effect of the 17¹ side chains, leads to a structure where the electronic coupling is high, even when the spatial overlap is less. Additionally, the coordinative bonds rigidify the structure, resulting in considerably reduced structural disorder compared to the DLC porphyrins. The importance of the zinc–oxygen coordination for maintaining an ordered structure in the ZnChls is illustrated in Figure 3, where the conductivity signal for ZnChl 1-OH is compared to that for the corresponding free base chlorin 1'-OH. While 1-OH gives a long living signal corresponding to a reasonable mobility (0.07 cm² V⁻¹ s⁻¹), the 1'-OH gives no measurable conductivity signal after the pulse. We attribute this to a disordered structure when the coordination bond is absent.

The distinct supramolecular organization that gives rise to different mobilities in the OH and OMe ZnChls also results in substantially different decay kinetics, as shown in Figure 4. The decay of the radiation-induced conductivity of ZnChls 1-OH and 1-OMe is plotted for different irradiation doses (i.e., different pulse duration) in Figure 4. Different irradiation doses

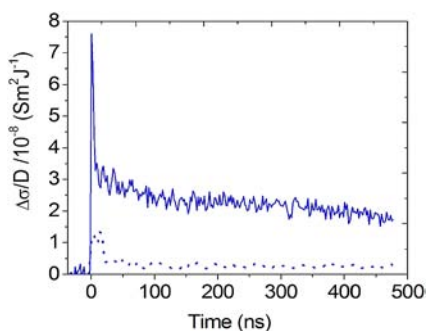


Figure 3. Transient change in conductivity for zinc chlorin 1-OH (solid line) and the corresponding free base chlorin 1'-OH (dotted line) upon irradiation with 10 ns electron pulse.

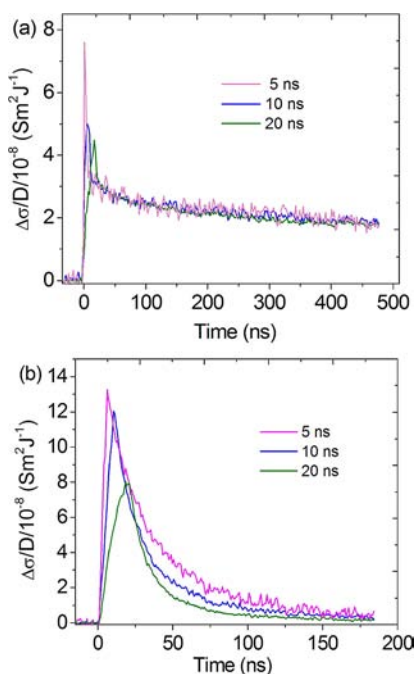


Figure 4. Transient change in conductivity for (a) 1-OH and (b) 1-OMe for different electron pulse durations.

result in different initial concentrations of charges. For 1-OH, the decay does not depend on the concentration of the charge carriers, and the half-life is of the order of a few microseconds (Figure 4a). Similar long lifetimes have been observed previously for DLCs,³¹ which form 1D stacks of aromatic cores that are surrounded by hydrophobic side chains. Although the arrangement of the stacks in the tubular structures formed by the OH compounds is more complex than in DLCs, a similar decay mechanism of the charge carriers is operative in the present case; i.e., the decay of the conductivity can be attributed to slow trapping of charge carriers and subsequent recombination via tunneling through the peripheral insulating hydrocarbon mantle around the tube.³³

In the conductivity transients of the OMe ZnChls, second-order recombination effects are present (Figure 4b); i.e., the rate of decay of the conductivity is sensitive to the initial concentration of charges. In this case, the much faster moving charges recombine on the time scale of ten(s) of nanoseconds. This is attributed to second-order effects that are known to be more pronounced in 2D and 3D networks, but not in 1D

columnar stacks.³⁴ This is consistent with the brickwork-type 2D structural arrangement of OMe compounds shown by solid-state NMR measurements,²⁰ where the interactions between neighboring stacks are presumably more important than in the OH compounds.²⁰

To gain more insight into the thermal stability and the temperature dependence of the conductivity, PR-TRMC measurements were performed between -50 and 100 °C. For the OH compounds the charge carrier mobilities were found to increase gradually with temperature, indicating thermally activated transport of charge carriers (Figure S1, Table S1). Moreover, changes in the magnitude of the conductivity are reversible for these compounds, indicating a thermally stable supramolecular organization of the ZnChls. However, the half-life time of the conductivity transients reduces significantly upon annealing, from microseconds to hundreds of nanoseconds. We conclude from this that the primary tubular structure of the aggregates that is formed in solution is maintained, and only the interactions between the neighboring alkyl chains surrounding the tubes are influenced by heating. In accordance with this interpretation, differential scanning calorimetry (DSC) shows no phase transitions in the OH compounds.

For the OMe compounds, the charge transport behavior on heating is very different. Heating the samples to 100 °C leads to an irreversible collapse of the conductivity signals (Figure S2). This suggests that the initial supramolecular structures of the OMe ZnChls formed in solution, although favorable for charge transport, are metastable in the solid state, and considerable change in the morphology occurs upon heating. To confirm this notion, we investigated the thermotropic behavior of 1-OMe by optical polarization microscopy (OPM) and DSC. Indeed the DSC thermogram reveals distinct differences for the first and subsequent heating–cooling cycles (Figure S3). Thus, while the second and third heating–cooling cycles are identical, the first heating process is different, which corroborates that 1-OMe molecules exhibit different packing arrangements upon self-assembly from solution and upon cooling from the melt. For the latter case our OPM and DSC investigations indicate the formation of a soft crystalline phase. Upon cooling from the melt (~ 170 °C), two phase transitions at 155 °C (-19.7 kJ/mol) and 69.8 °C (-10.5 kJ/mol) were observed (Figure S3). OPM studies revealed concomitant formation of spherulitic textures (Figure S4). These studies are indicative of substantial temperature-dependent changes in the morphology of the sample which are detrimental to charge transport.

In conclusion, efficient charge transport has been observed in semisynthetic ZnChl assemblies. Brickwork-type 2D stacked assemblies of 3¹-methoxy ZnChls possess very high charge carrier mobility of up to 0.28 cm² V⁻¹ s⁻¹ at room temperature, whereas corresponding tubular assemblies of 3¹-hydroxy ZnChls possess charge carrier mobility of up to 0.07 cm² V⁻¹ s⁻¹, revealing a clear relationship between supramolecular structure and charge transport properties of these biomimetic materials. In concordance with the high charge carrier mobilities of well-ordered ZnChl aggregates, these biomimetic materials possess potential for application in supramolecular electronics. Utilization of these dye assemblies, for instance, in field effect transistor fabrication³⁵ is conceivable.

■ ASSOCIATED CONTENT**■ Supporting Information**

Experimental methods; additional PR-TRMC transients; temperature-dependent mobility data for OH compounds; OPM and DSC data. This material is available free of charge via the Internet at <http://pubs.acs.org>.

■ AUTHOR INFORMATION**Corresponding Author**

wuerthner@chemie.uni-wuerzburg.de; f.c.grozema@tudelft.nl

Present Addresses

[#]Center for Nanofabrication and Molecular Self-Assembly, Department of Chemistry, Northwestern University, Evanston, IL

[§]Nano Organic Chemistry and Optoelectronic Materials Section, Department of Chemical Engineering, Delft University of Technology, Delft, The Netherlands

Notes

The authors declare no competing financial interest.

■ ACKNOWLEDGMENTS

This work was supported by a VENI grant to F.C.G. from the Netherlands Organization for Scientific Research (NWO). We thank the Bavarian State Ministry of Science, Research, and the Arts for funding the research at the Center for Nanosystems Chemistry at the University of Würzburg within the framework of the Collaborative Research Network "Solar Technologies Go Hybrid".

■ REFERENCES

- (1) Schenning, A. P. H. J.; Meijer, E. W. *Chem. Commun.* **2005**, 3245–3258.
- (2) Percec, V.; Glodde, M.; Bera, T. K.; Miura, Y.; Shiyonovskaya, I.; Singer, K. D.; Balagurusamy, V. S. K.; Heiney, P. A.; Schnell, I.; Rapp, A.; Spiess, H.-W.; Hudson, S. D.; Duan, H. *Nature* **2002**, *419*, 384–387.
- (3) Aida, T.; Meijer, E. W.; Stupp, S. I. *Science* **2012**, *335*, 813–817.
- (4) Kumar, S. *Liq. Cryst.* **2005**, *32*, 1089–1113.
- (5) Wu, J. S.; Pisula, W.; Müllen, K. *Chem. Rev.* **2007**, *107*, 718–747.
- (6) Chu, C. C.; Raffy, G.; Ray, D.; Del Guerso, A.; Kauffmann, B.; Wantz, G.; Hirsch, L.; Bassani, D. M. *J. Am. Chem. Soc.* **2010**, *132*, 12717–12723.
- (7) Sakai, N.; Sisson, A. L.; Buergi, T.; Matile, S. *J. Am. Chem. Soc.* **2007**, *129*, 15758–15759.
- (8) Wasielewski, M. R. *Acc. Chem. Res.* **2009**, *42*, 1910–1921.
- (9) Zhang, W.; Jin, W.; Fukushima, T.; Saeki, A.; Seki, S.; Aida, T. *Science* **2011**, *334*, 340–343.
- (10) Babu, S. S.; Prasanthkumar, S.; Ajayaghosh, A. *Angew. Chem., Int. Ed.* **2012**, *51*, 1766–1776.
- (11) Prasanthkumar, S.; Saeki, A.; Seki, S.; Ajayaghosh, A. *J. Am. Chem. Soc.* **2010**, *132*, 8866–8867.
- (12) Charvet, R.; Yamamoto, Y.; Sasaki, T.; Kim, J.; Kato, K.; Takata, M.; Saeki, A.; Seki, S.; Aida, T. *J. Am. Chem. Soc.* **2012**, *134*, 2524–2527.
- (13) Martinez-Planells, A.; Arellano, J. B.; Borrego, C. A.; López-Iglesias, C.; Gich, F.; Garcia-Gil, J. S. *Photosynth. Res.* **2002**, *71*, 83–90.
- (14) Montaña, G. A.; Bowen, B. P.; LaBelle, J. T.; Woodbury, N. W.; Pizziconi, V. B.; Blankenship, R. E. *Biophys. J.* **2003**, *85*, 2560–2565.
- (15) Savikhin, S.; Zhu, Y. W.; Blankenship, R. E.; Struve, W. S. *J. Phys. Chem.* **1996**, *100*, 3320–3322.
- (16) Prokhorenko, V. I.; Steensgaard, D. B.; Holzwarth, A. F. *Biophys. J.* **2000**, *79*, 2105–2120.
- (17) Saga, Y.; Akai, S.; Miyatake, T.; Tamiaki, H. *Bioconjugate Chem.* **2006**, *17*, 988–994.

- (18) Prokhorenko, V. I.; Holzwarth, A. R.; Müller, M. G.; Schaffner, K.; Miyatake, T.; Tamiaki, H. *J. Phys. Chem. B* **2002**, *106*, 5761–5768.
- (19) Brune, D. C.; Nozawa, T.; Blankenship, R. E. *Biochemistry* **1987**, *26*, 8644–8652.
- (20) Ganapathy, S.; Sengupta, S.; Wawrzyniak, P. K.; Huber, V.; Buda, F.; Baumeister, U.; Würthner, F.; de Groot, H. J. M. *Proc. Natl. Acad. Sci. U.S.A.* **2009**, *106*, 11472–11477.
- (21) Huber, V.; Katterle, M.; Lysetska, M.; Würthner, F. *Angew. Chem., Int. Ed.* **2005**, *44*, 3147–3151.
- (22) Huber, V.; Lysetska, M.; Würthner, F. *Small* **2007**, *3*, 1007–1014.
- (23) Huber, V.; Sengupta, S.; Würthner, F. *Chem.—Eur. J.* **2008**, *14*, 7791–7807.
- (24) Sengupta, S.; Ebeling, D.; Patwardhan, S.; Zhang, X.; von Berlepsch, H.; Böttcher, C.; Stepanenko, V.; Uemura, S.; Hentschel, C.; Fuchs, H.; Grozema, F. C.; Siebbeles, L. D. A.; Holzwarth, A. R.; Chi, L.; Würthner, F. *Angew. Chem., Int. Ed.* **2012**, *51*, 6378–6382.
- (25) Uemura, S.; Sengupta, S.; Würthner, F. *Angew. Chem., Int. Ed.* **2009**, *48*, 7825–7828.
- (26) Tamiaki, H.; Amakawa, M.; Shimono, Y.; Tanikaga, R.; Holzwarth, A. R.; Schaffner, K. *Photochem. Photobiol.* **1996**, *63*, 92–99.
- (27) Patwardhan, S.; Sengupta, S.; Würthner, F.; Siebbeles, L. D. A.; Grozema, F. C. *J. Phys. Chem. C* **2010**, *114*, 20834–20842.
- (28) Grozema, F. C.; Siebbeles, L. D. A. *Int. Rev. Phys. Chem.* **2008**, *27*, 87–138.
- (29) Spano, F. C. *Acc. Chem. Res.* **2010**, *43*, 429–439.
- (30) Warman, J. M.; de Haas, M. P.; Dicker, G.; Grozema, F. C.; Piris, J.; Debije, M. G. *Chem. Mater.* **2004**, *16*, 4600–4609.
- (31) Warman, J. M.; Van de Craats, A. M. *Mol. Cryst. Liq. Cryst.* **2003**, *396*, 41–72.
- (32) van de Craats, A. M.; Warman, J. M.; Fechtenkötter, A.; Brand, J. D.; Harbison, M. A.; Müllen, K. *Adv. Mater.* **1999**, *11*, 1469–1472.
- (33) Warman, J. M.; Piris, J.; Pisula, W.; Kastler, M.; Wasserfallen, D.; Müllen, K. *J. Am. Chem. Soc.* **2005**, *127*, 14257–14262.
- (34) Grassberger, P.; Procaccia, I. *J. Chem. Phys.* **1982**, *77*, 6281–6284.
- (35) Beaujuge, P. M.; Fréchet, J. M. J. *J. Am. Chem. Soc.* **2011**, *133*, 20009–20029.